Smart Structures and Systems, Vol. 6, No. 1 (2010) 57-72
DOI: http://dx.doi.org/10.12989/sss.2010.6.1.057

Small scale experimental testing to verify the effectiveness of the base isolation and tuned mass dampers combined control strategy

Luigi Petti*, Giovanni Giannattasio‡, Massimiliano De Iuliis‡† and Bruno Palazzo‡‡

Department of Civil Engineering, University of Salerno, Via Ponte don Melillo 84084 Fisciano (SA), Italy

(Received December 31, 2008, Accepted July 11, 2009)

Abstract. This paper presents the most significant results obtained within a broad-ranging experimental program aiming to evaluate both the effectiveness and the robustness of a Base Isolation (BIS) and a Tuned Mass Damper (TMD) combined control strategy (BI & TMD). Following a brief description of the experimental model set-up and the adopted kinematic scaling technique, this paper describes the identification procedures carried out to characterize the system's model. The dynamic response of a small-scale model to recorded earthquake excitations, which has been scaled by using the Buckingham pi-theorem, are later presented and discussed. Finally, the effectiveness and robustness of the combined control strategy is evaluated by comparing the model's dynamic response. In particular, reduction in relative displacements and absolute accelerations due to the application of different mass damping systems is investigated.

Keywords: small scale model; vibration control; base isolation; tuned mass damping.

1. Introduction

As is well-known, the effectiveness of a base isolation system (BIS) depends on its filtering capacity over the range of frequencies where the seismic energy is higher. The BIS acts as a low-pass filter which reduces the amplitude of signals with energy content concentrated on frequencies close to those of the isolation system (cutoff frequency) (Palazzo and Petti 1997). However, filtering action has, on occasions, to be applied to an unpredictable excitation having random dynamic characteristics. It is known that even when detailed data from previous seismic events are available, the hazard should be derived from more than one seismic source and it is impossible to define a single earthquake scenario that is compatible with the results of probabilistic seismic hazard assessment (Bommer, *et al*. 2000). Therefore, it is clear that the first natural frequency can never shift out of the "possible" energy content frequency range for any type of seismic excitation. This causes BIS structures, under unfavorable seismic excitations, to produce very high displacements at the base.

With this in mind, Palazzo and Petti (1994), proposed a new, combined control system based on the application of mass damping on the isolation layer in a base isolated structure. The idea of a new hybrid

*Assistant Professor, Correspondence Author, E-mail: petti@unisa.it
‡PhD student
‡†Research Assistant
‡‡Full Professor

system, based on a combination of the Tuned Mass Damper strategy and Base Isolation (BI & TMD), came from the observation that the response of well-isolated systems is dominated by the first-modal contribution and that TMD is able to reduce solely that fundamental vibration mode. In fact TMD acts as a band-pass filter which only allows for the passage of frequencies within a certain range. The objective is to protect the BIS from those excitation components, which are close to the natural vibration frequency, by controlling the amplitude of the fundamental modal contribution due to the satellite TMD action installed on the base isolation layer. Previous works have positively investigated the effectiveness and robustness respect to the input signal of the proposed strategy by means of numerical experimentation on both bi-dimensional (Palazzo and Petti 1994) and tri-dimensional (Palazzo, *et al.* 2006) structural models.

Within this context, the present paper aims to investigate mass damping effectiveness and robustness in reducing the relative seismic displacement at isolation level and its effect on the dynamic behavior of the superstructure by performing a broad-ranging experimental program on a small-scale, three-degree of freedom model, representing the translational dynamic behavior of a combined BI & TMD system.

After a brief introduction concerning BI & TMD control strategy principia, this paper goes on to describe model identification both for single elements and the whole system, carried out by using numerical procedures based on floating mean regressive processes. The dynamic behavior of the model was successively analyzed when subjected to different recorded time-history accelerations corresponding to seismic events having very different magnitudes and energy content. Model and tests have been designed by considering a kinematic scaling technique based on the application of the Buckingham pi-theorem.

The results obtained allow for an evaluation of combined strategy effectiveness and robustness by comparing the seismic response of the model with and without the application of the mass damper at the isolation layer.

2. BI & TMD control strategy principia

Let us consider the three-degree of freedom mathematical representation of the combined BI & TMD system shown in Fig. 1.

Given that ω_b and ξ_b, ω_{is} and ξ_{is}, ω_T and ξ_T are the natural frequencies and the damping factors of the superstructure, isolation and TMD, respectively, the motion equations of the system can be written as:

$$\begin{aligned} \ddot{u} + 2\xi_T\omega_T\dot{u} + 2\omega_T^2 u &= 2\xi_T\omega_T\dot{u}_{is} + \omega_T^2 u_{is} \\ \ddot{x}_b + 2\xi_b\omega_b\dot{x}_b + \omega_b^2 x_b &= -\ddot{u}_{is} \\ \ddot{u}_{is} + 2\xi_{is}\omega_{is}\dot{u}_{is} + \omega_{is}^2 u_{is} &= 2\xi_{is}\omega_{is}\dot{u}_g + \omega_{is}^2 u_g - \mu\ddot{u} - \chi\ddot{x}_b \end{aligned} \tag{1}$$

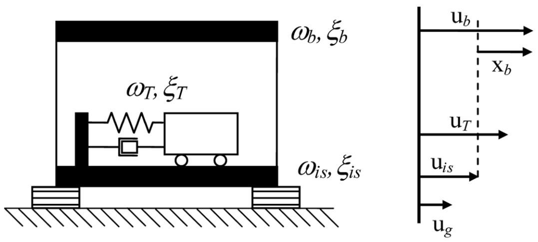

Fig. 1 Base isolated system provided with TMD

where μ and χ indicate the two mass ratios $\mu = m/(m_b + m_{is})$ and $\chi = m_b/(m_b + m_{is})$. By operating the Laplace transforms and organizing them, we obtain:

$$
\begin{aligned}
U &= G(s)U_{is} \\
X_b &= H_b(s)U_{is} \\
U_{is} &= G_{is}(s)U_g + G_{is}(s)\frac{-s^2\mu}{2\xi_{is}\omega_{is}s + \omega_{is}}U + B(s)X_b
\end{aligned}
\tag{2}
$$

in which the following transfer functions are introduced: $G(s) = \dfrac{2\xi_T\omega_T s + \omega_T^2}{s^2 + 2\xi_T\omega_T s + \omega_T^2}$, $H_b(s) = \dfrac{-s^2}{s^2 + 2\xi_b\omega_b s + \omega_b^2}$, $G_{is}(s) = \dfrac{2\xi_{is}\omega_{is}s + \omega_{is}^2}{s^2 + 2\xi_{is}\omega_{is}s + \omega_{is}^2}$, $B(s) = \dfrac{-\chi s^2}{s^2 + 2\xi_{is}\omega_{is}s + \omega_{is}^2}$. Even in this case, regarding well-designed systems, we can show the insignificant influence of the interaction term $B(s)X_b$ and therefore Eq. (2) becomes (Palazzo and Petti 1997):

$$
U_{is} \cong G_{is}(s)U_{ig} + G_{is}(s)\alpha(s)U \tag{3}
$$

with $\alpha = \dfrac{-s^2\mu}{2\xi_{is}\omega_{is}s + \omega_{is}}$, and thus we obtain:

$$
X_b = \frac{G_{is}(s)}{1 + G_{is}(s)\alpha(s)G(s)} \cdot H_b(s) \cdot U_g \tag{4}
$$

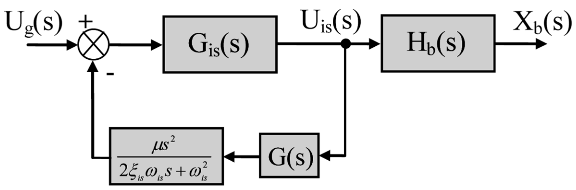

Fig. 2 Block diagram of the combined control system “Base Isolation + TMD”

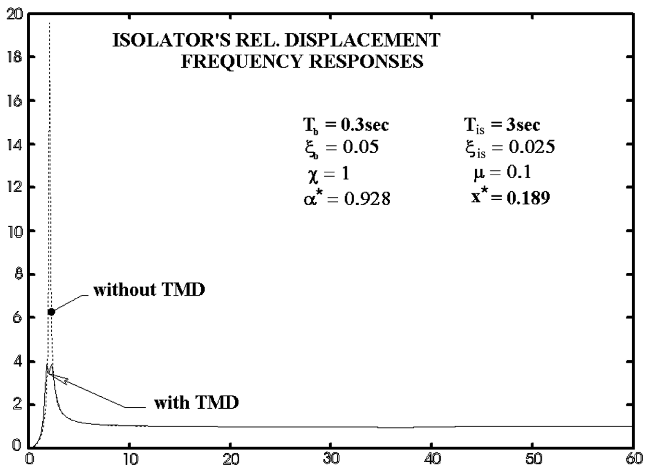

Fig. 3 TMD function principle (α^* optimal tuning ratio)

which corresponds to the control scheme shown in Fig. 2.

As the block diagram clearly shows, the isolation level works as an open-loop control protecting the superstructure. The main drawback of this control scheme is that it is unable to adapt to the structural response, unlike the TMD which works as a feedback control, using the energy of the structural response to prevent high-displacement seismic demand in the isolation bearings.

Finally, the transfer functions plotted in Fig. 3 (Palazzo and Petti 1997) show how the effect of TMD, reduction of amplification in a narrow band, favorably combines with BIS because, as is well-known, the fundamental mode is highly dominant in isolated systems.

3. Description of the small-scale model and the experimental set-up

To study the effectiveness and robustness of the BI & TMD combined control strategy, a small-scale model was adopted (Fig. 4), representing a three-degree of freedom system designed by using a kinematic scaling technique. The model results from the assembling of different sub-systems, whose dynamic responses can be described by using the classical SDOF mathematical formulation:

$$\ddot{x}(t) + \frac{4\pi\xi\dot{x}(t)}{T_0} + \frac{4\pi^2 x(t)}{T_0^2} = -\ddot{y}(t) \tag{5}$$

where $\ddot{x}, \dot{x}$ and x respectively represent acceleration, velocity and displacement, T_0 and ξ the natural period and the damping factor, and $\ddot{y}$ the seismic input acceleration. The dynamic response of each sub-system can be implicitly stated as:

$$x = f(t, T_0, y, \xi) \tag{6}$$

By applying the Buckingham pi-theorem (Dove and Bennett 1986), after having set the structural damping factor, the previous expression can be modified in a dimensionless form:

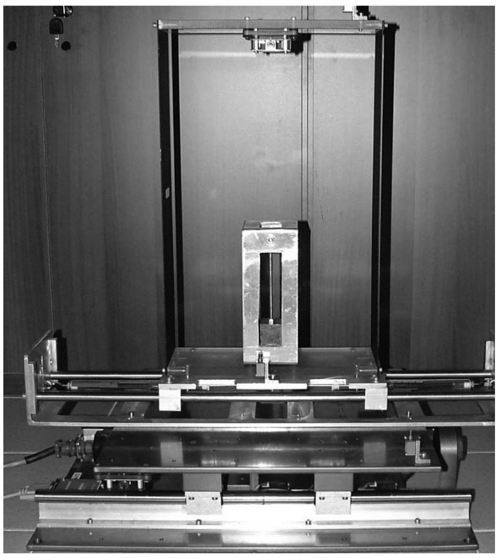

Fig. 4 Small scale model

$$\pi_1 = \Phi(\pi_2) \tag{7}$$

with π_1 and π_2 dimensionless parameters respectively equal to $\ddot{y}/\ddot{x}$ and $x/(t^2 \cdot \ddot{x})$. This statement, formally represented by Eq. (7), is independent of the actual physical dimensions of the systems being studied and allows for total kinematic similarity. This means that the data relating to directions and velocity in the actual, full-scale system is proportionately identical to the data relating to the small-scale system.

This scaling approach is extremely appropriate in investigating the effectiveness and robustness of BI & TMD combined control strategy by considering structural performance in terms of two kinematic parameters: relative displacement at the isolation layer and the absolute acceleration of the superstructure.

The parameters adopted to define scale ratios within this framework are time (t), and acceleration ($\ddot{y}$), in particular being N_t and $N_{\ddot{y}}$ respectively the scale ratio for time and acceleration. The scale factor for length N_L is therefore defined as:

$$N_t = \overline{N_t};\ N_{\ddot{y}} = \overline{N_{\ddot{y}}};\ N_L = \overline{N_{\ddot{y}}} \cdot \overline{N_t^2} \tag{8}$$

This methodology allows us to explore the dynamic behavior of a class of real full-scale structures (Sonin 1997), characterized by their fundamental periods, by using the same scaled model and only varying the time scale ratio.

In the following, the three sub-systems composing the small-scale model are described:

- A single-level framed system (Quanser Inc.), corresponding to the superstructure. This is made up of two vertical steel elements, 500 mm high with a 1.75×101.1 mm rectangular section, and by a polystyrene horizontal element, wide 310 mm and with a 11×110 mm section. The framed system has a fundamental vibration period of 0.27 sec;
- A Base Isolation system on rails lines, arranged by using a 6 mm thin aluminum supporting plate having significant axial and flexural stiffness and two 14 mm diameter circular rods on which the abovementioned plate can slide by means of four ball bearings. Two dynamometers, acting in parallel, are also installed to provide a suitable degree of isolation. The BIS system presents a fundamental vibration period of 0.49 sec (Figs. 5-6);
- A Tuned Mass Damper realized by using a pendulum system (Fig. 7), made of a 195×100 mm aluminum box-shaped element having 4 mm thickness. The oscillating mass, with 10% mass ratio, consists of a 30 mm cubic element and its position can be modified in order to change the pendulum

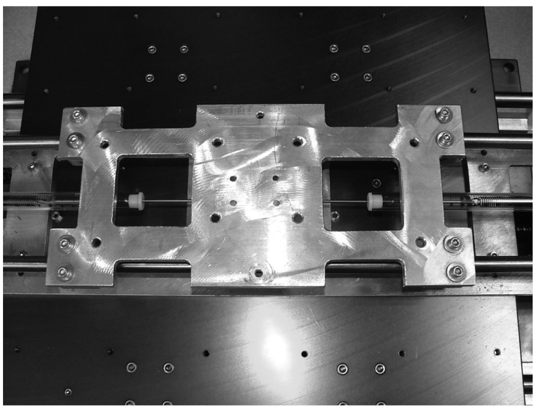

Fig. 5 Base isolation system

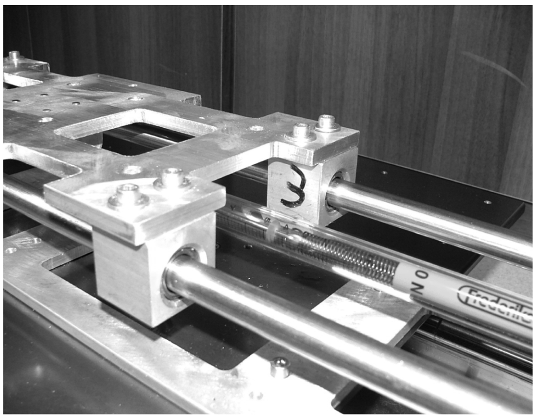

Fig. 6 Detail of the base isolation system

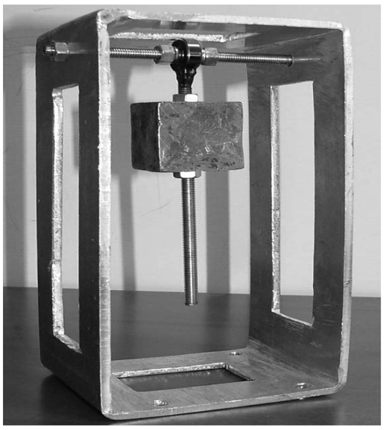

Fig. 7 TMD system

Table 1 Accelerometer's characteristics

	Quanser Inc.	PCB Piezotronics Inc.
Accelerometer range	± 5 g	± 3 g
Voltage sensitivity	1000 mV/g	1000 mV/g
Resolution	0.001 g	0.00003 g

period in the range 0.28 to 0.77 sec.

The system can be easily disassembled, allowing for the investigation of the dynamic behavior concerning different model configurations: fixed base system, base isolated system, base isolated and tuned mass damping system.

Experimental tests were carried out by using a single degree of freedom shaking table "Shake Table 2" (Kravchuk, *et al*. 2008, Battaini, *et al*. 1999) manufactured by "Quanser Consulting" (Quanser Inc., Dyke and Caicedo 2002).

During the tests, the shake table, base isolation and framed system accelerations were constantly monitored by using two different accelerometer typologies, whose features are listed in Table 1, in order to obtain reliable control of the measurable variable values.

Signal data were captured by using the acquisition card provided by Quanser Inc., DAC Q4 with extension card ETC Q4 (Dyke, *et al.* 2006, 2007) and the PCB accelerometer data acquisition was carried out by means of a 16 analogue input-channels DAQPad-6015 board by National Instruments, capable of 16-bit sequential sampling.

4. Identification procedure

In order to perform dynamic identification of the small-scale model, the linear dynamic response of the system was described by using the following mathematical representation:

$$y(t) = G(q) \cdot u(t) + H(q) \cdot e(t) \tag{9}$$

where $G(q)$ and $H(q)$ represent the system's transfer functions relating the response respectively to the input signal $u(t)$ and the noise $e(t)$, whereas q represents a time-shift math operator. The $G(q)$ and $H(q)$ transfer functions were estimated by using an ARMAX (AutoRegressive Moving Average with eXtra

Table 2 Summary of identification results

System		T (s)	x (%)
Fixed framed system		0.28	0.90
Base isolation		0.49	4.40
Base isolation system	1st mode	0.77	4.65
	2nd mode	0.23	18.32
BI & TMD	1st mode	0.98	5.30
	2nd mode	0.66	8.17
	3rd mode	0.23	11.85

input) (Ljung 1999) procedure, based on a floating mean regressive process, using the following equation:

$$A(q)\cdot y(t) = B(q)\cdot u(t) + C(q)\cdot e(t) \tag{10}$$

where $A(q)$, $B(q)$ and $C(q)$ are three polynomial terms.

This identification procedure aims to evaluate numerically the parameters of the system so that the dynamic response of the small-scale model fits with the experimental measurement data. The choice of best order for polynomial terms was done with a computational iterative procedure in Matlab (Ljung 2007). With this aim in mind, a multi-sine input signal was adopted as input signal:

$$u(t) = \sum_{k=1}^{d} a_k \cos(\omega_k t + \varphi_k) \tag{11}$$

This signal allowed the researchers to check the amount of input energy to the analyzed system within a pre-assigned frequency range. Moreover, a phase angle distribution, φ_k, allowed us to limit the crest factor value, in order to make the dynamic response amplitude stay within the physical limits of the shake table. Schroeder (1970) proposed the following distribution:

$$\varphi_k = \varphi_1 - \frac{k(k-1)}{d}\pi \quad 2 \le k \le d \tag{12}$$

where φ_1 is an arbitrary phase angle value and "k" is an index referring to sine function circular frequency and amplitude (Eq. (12)). The multi-sine input used in the identification procedure had the

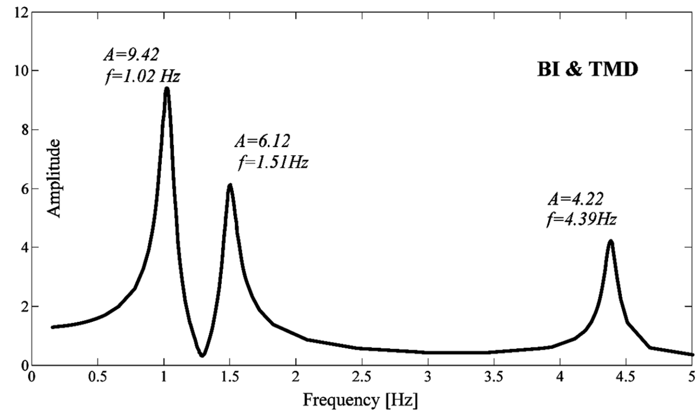

Fig. 8 Transfer function: magnitude

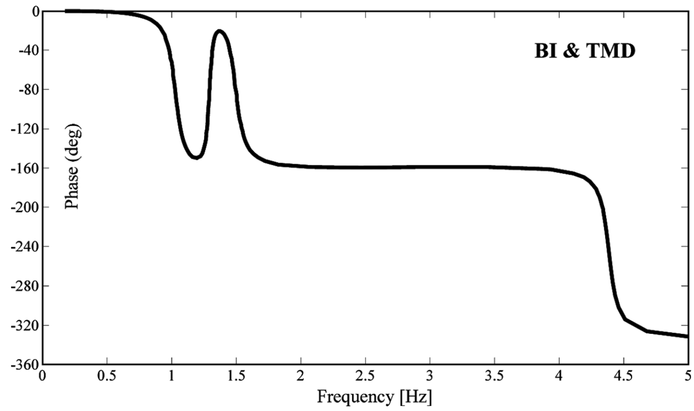

Fig. 9 Transfer function : phase diagram

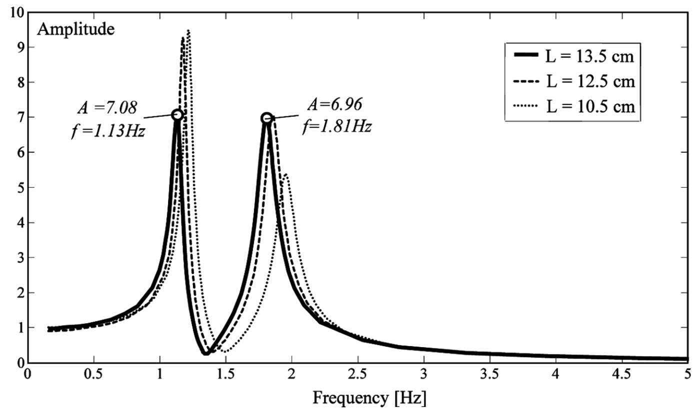

Fig. 10 TMD tuning effects – TF magnitude

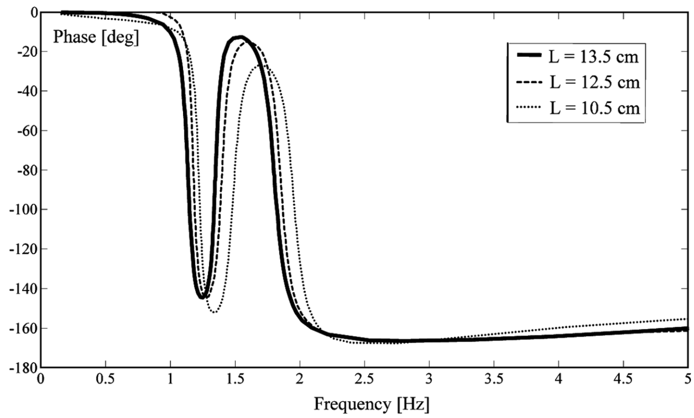

Fig. 11 TMD tuning effects – TF phase diagram

following parameters: $d = 76$ (number of the sinusoidal components), frequency range = 0.1÷7.5 Hz (frequency step = 0.1 Hz), $a_k = 1$ cm, $\varphi_1 = 0$ rad.

In Figs. 8-9, the results of the identification procedure for the BI & TMD system are plotted in terms of transfer function (TF) magnitude and phase diagram. Figs. 10-11 show the effect of different TMD tuning, obtained by modifying the pendulum length L, on the systems' frequency response. In Table 2, the results concerning the identification procedures for each single analyzed sub-system are summarized.

The results, obtained by using the ARMAX approach, were also positively compared with results deriving from different identification procedures. In particular, a 1% to 2% difference between the ARMAX approach results and free vibration procedure results were observed for fixed base (T_{Free} = 0.27 sec - T_{ARMAX} = 0.28 sec) and base isolation (T_{Free} = 0.49 sec - T_{ARMAX} = 0.49 sec) systems. Similar differences are also obtained in the case of Base Isolated systems with and without Tuned Mass Damper.

5. Experimental test results

The small-scale model, in base-isolated configuration with and without TMD, was tested by using scaled recorded accelerograms, corresponding to seismic events which have taken place in Europe and also adopted for research purposes within a National Italian Research Project named ReLUIS (Rete dei Laboratori Universitari di Ingegneria Sismica).

In Table 3, the main features of the considered seismic events are listed, while, for some of them, absolute acceleration and relative displacement spectra are plotted in Figs. 12-13. In Table 4 the investigated fundamental period range and the corresponding scaling factor for every input signal are reported. In particular, parameter N_t was chosen in order to investigate a suitable fundamental period range for base

Table 3 Seismic events considered

Seismic events	Date of Reg.	Earth. Cod.	Rec. Time
Belgrade	15/04/1979	0196X,0196Y	48.23 s
Belgrade	15/04/1979	0199X,0199Y	47.82 s
Belgrade	15/04/1979	0228X,0228Y	34.35 s
Italy	23/11/1980	0288X 0288Y	30.16 s 73.21 s
Ankara	13/03/1992	0535X,0535Y	21.28 s
Iceland	21/06/2000	6328X,6328Y	51.37 s

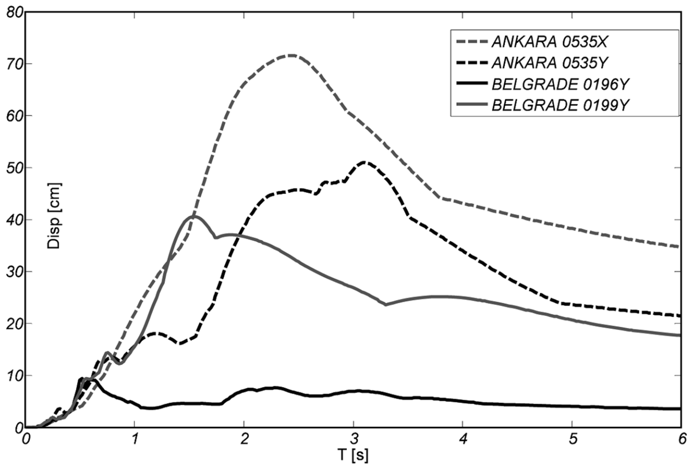

Fig. 12 Seismic events displacement spectra

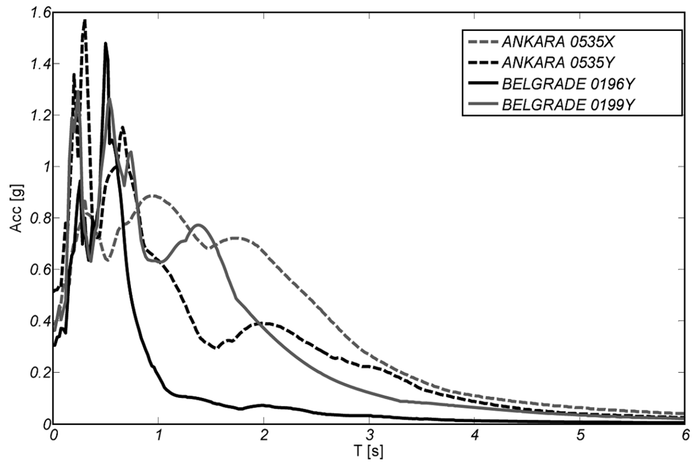

Fig. 13 Seismic events acceleration spectra

Table 4 Considered scale factors and fundamental period range

Earth. Cod.	T_{BIS} (s)	N_t (-)	$N_{\ddot{y}}$ (-)
Belgrade 0196X	0.75 ÷ 4.00	1.01 ÷ 5.39	4.90 ÷ 0.15
Belgrade 0196Y	0.75 ÷ 4.00	1.01 ÷ 5.39	2.40 ÷ 0.12
Belgrade 0199X	0.75 ÷ 4.00	1.01 ÷ 5.39	5.50 ÷ 0.20
Belgrade 0199Y	0.75 ÷ 4.00	1.35 ÷ 5.39	2.75 ÷ 0.20
Belgrade 0228X	0.50 ÷ 4.00	0.67 ÷ 5.39	3.50 ÷ 0.10
Belgrade 0228Y	0.50 ÷ 4.00	0.67 ÷ 5.39	3.50 ÷ 0.13
Enel 0288X	0.75 ÷ 5.00	1.01 ÷ 6.73	2.00 ÷ 0.12
Enel 0288Y	1.25 ÷ 5.00	1.68 ÷ 6.73	0.65 ÷ 0.10
Ankara 0535X	1.00 ÷ 4.00	1.35 ÷ 5.39	5.00 ÷ 0.40
Ankara 0535Y	0.75 ÷ 4.00	1.01 ÷ 5.39	5.00 ÷ 0.28
Iceland 6328X	0.75 ÷ 5.00	1.01 ÷ 6.73	2.00 ÷ 0.15
Iceland 6328Y	0.75 ÷ 5.00	1.01 ÷ 6.73	2.40 ÷ 0.20

isolated systems ($N_t = T_{real}/T_{scaled}$), whereas parameter $N_{\ddot{y}}$ was selected to both accomplish the shake table displacement and velocity limits and control the environmental noise contaminating the measured variables. Within the parametric analysis, the period step, referring to the real system scale, was set as equal to $\Delta T_{BIS} = 0.25$ sec.

Results of the experimental tests are described in Figs. 14-15. In particular, these figures respectively show isolation level displacement and superstructure absolute acceleration spectra in the case of BIS and BI & TMD systems for three different recorded seismic events: Ankara 0535X, Ankara 0535Y and Belgrade 0196Y. Results show significant seismic response reduction in the first two cases: isolation level maximum relative displacement decreases from 66.04 cm to 50.80 cm for Ankara 0535X event and from 53.73 cm to 40.01 for Ankara 0535Y, the percentage reduction is therefore respectively equal to 23.08%, 25.53%.

This is mainly due to the spectral characteristics of the considered seismic events (Figs. 12-13). The

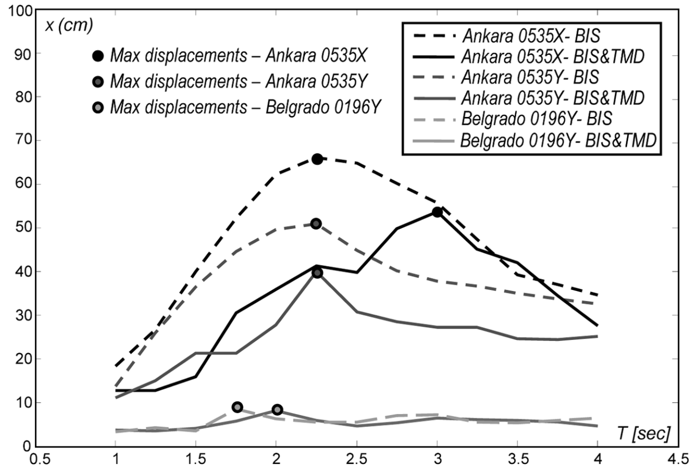

Fig. 14 Isolation level relative displacement spectra

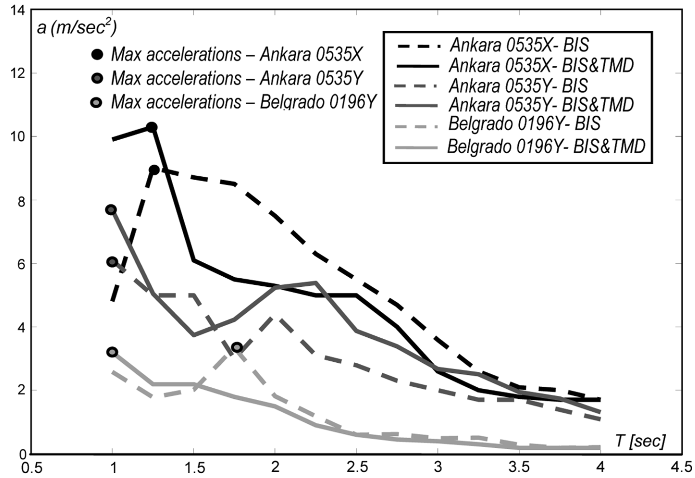

Fig. 15 Superstructure absolute acceleration spectra

abovementioned recorded excitations, in fact, present high energy content at low frequency, making the base isolation layer experience maximum displacement of the devices. In these cases the application of BI & TMD presents high performance level in reducing the seismic demand at the isolation layer, moreover the superstructure's seismic response showed low sensitivity to the application of mass damping strategy. The application of the TMD at the isolation layer allows the BIS strategy to be effective even in the case of unfavorable seismic excitations. In terms of control theory, it increases the robustness of the strategy with regard to the input signal.

In the case of the Belgrade 0196Y seismic event the installation of a TMD on the isolation layer does not produce a mitigation effect on seismic response. Maximum relative displacement is 8.22 cm for BIS and 8.61 cm after application of a mass damping system; moreover the acceleration of the superstructure also increases. However, these results have to be considered in the light of the purpose of BI & TMD combined control strategy. The Belgrade 0196Y seismic event, in fact, presents very limited energy content at low frequencies (Figs. 12-13), therefore the BIS strategy represents the most suitable approach

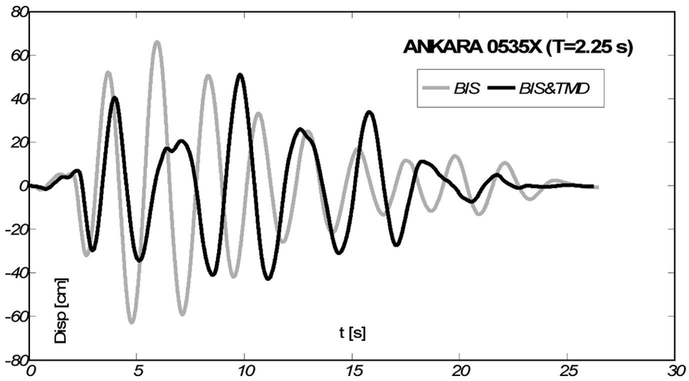

Fig. 16 Isolation layer relative displacement time history

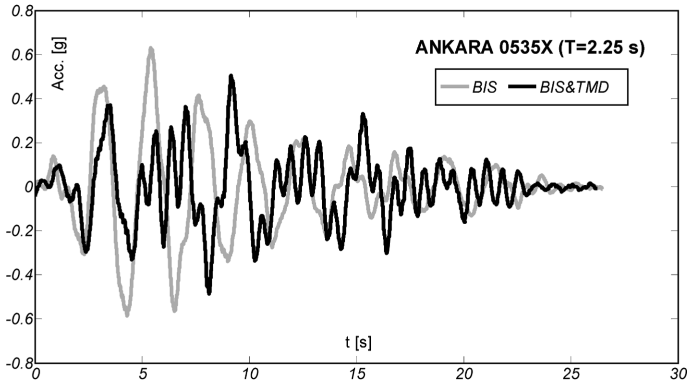

Fig. 17 Superstructure absolute acceleration time history

for controlling the seismic response. In fact, the isolator drift seismic demand stays within the allowable values for typical isolation devices, since the seismic energy is concentrated at frequencies beyond those fundamental frequencies of the structure. Similar results are obtained for the other considered seismic events, for which the abovementioned consideration still stands, however they showed how the seismic response of the isolation layer is rarely worsened by the application of a TMD even when BIS strategy works well, and that superstructure absolute acceleration doesn't significantly modify its values.

In Fig. 16 comparisons between isolation layer relative displacement time-history for BIS and BI & TMD systems, in the case of the Ankara0535X earthquake, has been plotted, while in Fig. 17 the same comparisons referring to superstructure absolute acceleration are shown.

In order to highlight the effectiveness and robustness of the proposed combined control strategy, an in-depth numerical analysis of the obtained results has been carried out. Firstly the following effectiveness indexes are defined:

$$\Delta x^{\%}(T) = \frac{1}{N}\sum_{i=1}^{N}\frac{x_{BIS,i}^{\max}(T) - x_{BIS\&TMD,i}^{\max}(T)}{x_{BIS,i}^{\max}(T)} \tag{13}$$

$$\Delta \ddot{x}^{\%}(T) = \frac{1}{N}\sum_{i=1}^{N}\frac{\ddot{x}_{BIS,i}^{\max}(T) - \ddot{x}_{BIS\&TMD,i}^{\max}(T)}{\ddot{x}_{BIS,i}^{\max}(T)} \tag{14}$$

representing the average reduction of the maximum system's isolation level seismic response by

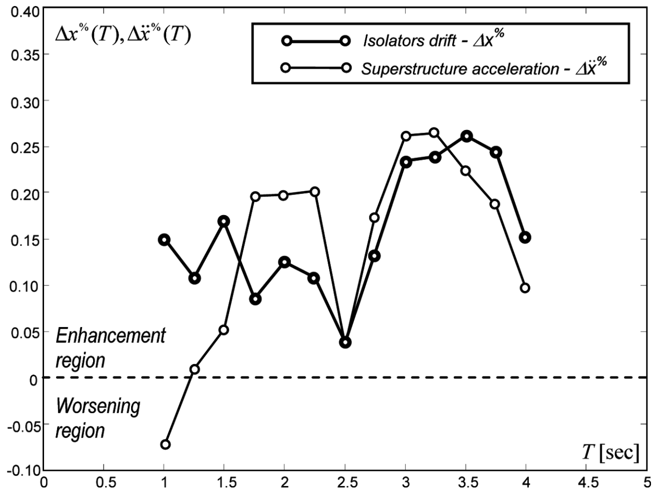

Fig. 18 Effectiveness indexes spectrum

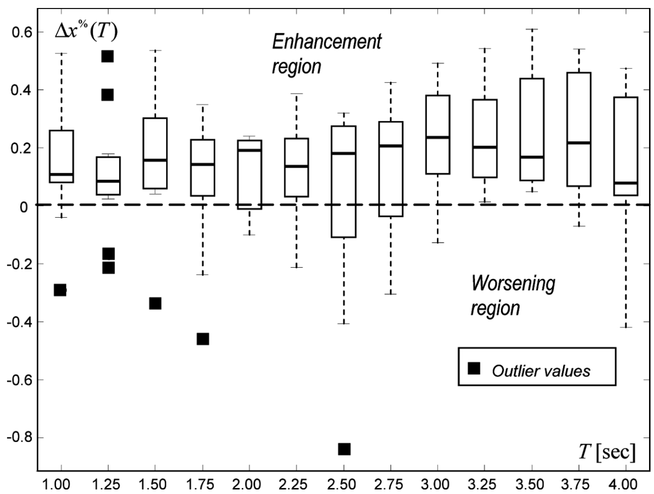

Fig. 19 Box plot representation of $\Delta y^{\%}$ index

considering the whole set of seismic excitations (index "i" refers to the different seismic inputs) and obtained by introducing the TMD at the isolation level as a function of the fundamental vibration period of the isolated system, T. In Fig. 18, these indexes are plotted on varying T, whereas in Fig. 19 the distribution of the percentage variation of isolators drift, on varying the seismic input is represented by using a box-plot diagram, in which five-number summaries: the smallest observation (minimum sample), lower quartile, median, upper quartile, and largest observation (maximum sample) are shown. Observed data on the interquartile range, which is more than 1.5 times lower than the first quartile or higher than the third quartile is considered as an outlier.

These figures clearly show the effectiveness of the proposed strategy when applied to structural systems subjected to a broad set of seismic excitations. In particular, a 10-15% average reduction of both isolator drift and superstructure acceleration has been observed (Fig. 18), moreover the statistical distribution of the seismic response shows that in more than 85% of the experimental tests the combined control strategy reduces the seismic demand at the isolation level (Fig. 19), with a maximum percentage reduction greater

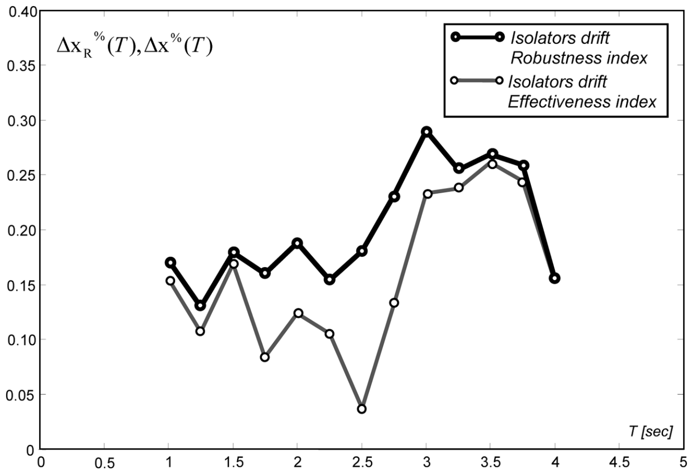

Fig. 20 Robustness index spectrum

than 60%. An interesting consideration on these results specifically concerns the outlier values of the statistical distribution. It has been observed that for one seismic excitation, namely Iceland6328X, the seismic response worsens by more than 80%. However, due to the dynamic characteristic of the seismic input, the maximum drift at the isolation level modifies from 6.05 cm to 11.13 cm, which is a value that is still compatible with the isolators' capacity limit.

Conversely, the positive outliers, representing better performances in reducing the isolators maximum drift have been observed for the following seismic events: Ankara0535X, Ankara0535Y, Belgrado 0199Y, Iceland6328Y, just right the seismic excitation having higher energy content on low frequencies. This means that the BIS&TMD system can be considered as an isolator drift robust control strategy with regard to the seismic input. However, such a feature is not perceptible by using the index defined in Eqs. (13)-(14) because every excitation is taken into consideration regardless of its hazard with respect to the BIS system.

In order to investigate the robustness of the combined strategy, the following index has also been considered:

$$\Delta x_R^{\%}(T) = \frac{1}{N}\sum_{i=1}^{N} p_{d,i} \cdot \frac{x_{BIS,i}^{\max}(T) - x_{BIS\&TMD,i}^{\max}(T)}{x_{BIS,i}^{\max}(T)} \tag{15}$$

in which $p_{d,i} = x_{BIS,i}^{\max} / \left(\sum_{j=1}^{N} x_{BIS,i}^{\max}\right)$ is a weight function evaluated by considering the maximum seismic response in terms of isolation level displacements. It intends to explicitly take into account the different hazard levels related to the seismic input considered. This allows us to have a synthetic representation of the control robustness, giving greater relevance to system performance in the case of unfavorable seismic inputs.

In Fig. 20, this index is compared with the unweighted one, as defined in Eq. (13).

Values of $\Delta x_R^{\%}$ index, and its comparison with $\Delta x^{\%}$, highlight the improvement in effectiveness of the BIS and TMD control strategy when seismic demand in terms of isolator displacement is greater. This is simply proven by looking at the robustness index values, which are in any case higher than the unweighted ones. Moreover, an average reduction, greater than 20% has been observed, and the new index spectrum assumes an almost flat shape, which represents two desirable design characteristics.

6. Conclusion

In the present paper, experimental tests on a small-scale model have been presented in order to investigate the effectiveness of the Base Isolation and Tuned Mass Damping combined control strategy. Previous theoretical studies have proved that this approach allows for protection of the isolation layer from unfavorable seismic events, without reducing the beneficial effects of the Base Isolation strategy to the superstructure dynamics.

The results of the experimental tests, carried out on a 3DOF small scale system, confirm both the effectiveness and sensitivity of the isolation system as a seismic protection technique. The possibility of improving its robustness by combining this technique with a mass damping passive control strategy is thus verified. In particular, the seismic response of the isolation layer is generally reduced by up to 40% in terms of maximum relative displacement in the case of an earthquake having high energy content at low frequencies and this should allow the devices to work properly, remaining within the displacement limit they are designed for, even if they experience an unfavorable seismic event.

Moreover, low absolute sensitivity of the superstructure's seismic response to the TMD system application has been observed. Finally, the isolation layer seismic response is rarely worsened by adding a well-designed mass damper on the isolation level, even when BIS strategy works well. The superstructure's absolute acceleration appears, in general, to be reduced when BIS and TMD strategy is considered. However, this tendency is inverted when unfavorable seismic events are considered, due to the negative effect of the TMD on the filtering action performed by the isolation level, without though, affecting the overall efficiency of the combined control strategy.

Acknowledgment

The authors are grateful to the ReLuis consortium for their support for our research activities.

References

Battaini, M., Yang, G. and Spencer Jr., B.F. (1999), "Bench-scale experiment for structural control", *J. Eng. Mech.* ASCE, **126**, 140-148.

Bommer, J.J., Scott, S.G. and Sarma, S.K. (2000), "Hazard-consistent earthquake scenarios", *Soil Dyn. Earthq. Eng.*, **19**(4), 219-231.

Dove, R.C. and Bennet, J.G. (1986), "Scale modeling of reinforced concrete category i structures subjected to seismic loading", *Mechanical/Structural Engineering Branch Division of Engineering Technology Office of Nuclear Regulatory Research U.S. Nuclear Regulatory Commission*, Washington, DC 20555.

Dyke, S.J. and Caicedo, J.M. (2002), "The university consortium on instructional shake tables", *Proc. of the ICANCEER Conf.*, Harbin, China, August.

Dyke, S.J., Jiang, Z., Christenson, R., Gao, X. and Courter, S. (2007), "Teleoperation and teleparticipation of instructional shake tables using the NEES cyberinfrastructure", *Proc. of the World Forum on Smart Materials and Smart Structures Technology,* Chongqing and Nanjing, May.

Dyke, S.J., Vaziri, P. and Roblee, C. (2006), "Execution of the Vision for NEES Education, Outreach and Training", *Proc. of the Int. Conf. on Engineering Education*, Puerto Rico, July.

Kravchuk, N., Colquhoun, R. and Porbaha, A. (2008), "Development of a friction pendulum bearing base isolation system for earthquake engineering education", *Proc. of the 2008 American Society for Engineering Education Pacific Southwest Annual Conf.*, Pittsburg, Pennsylvania, June.

Ljung, L. (1999), *System Identification: Theory for the User, II edition*, Prentice Hall, Upper Saddle River, N.J.

Ljung, L. (2007), *System Identification Toolbox 7 User's Guide, Revised for Version 7.1* (Release 2007b), The MathWorks, Inc.

Palazzo, B. and Petti, L. (1994), "Seismic response control in base isolated system using tuned mass dampers", *Proc. of First World Conf. on Structural Control*, Los Angeles, California, August.

Palazzo, B. and Petti, L. (1997), "Aspects of structural vibration passive control", *Meccanica*, **32**(6), 529-544.

Palazzo, B., Petti, L. and De Iuliis, M. (2006), "Tuned mass dampers to control the base-isolated benchmark building model", *Proc. of the 1st European Conf. on Earthquake Engineering and Seismology*, Geneve (CH), September.

Quanser Inc, "Shake Table II: User Manual – Revision 2", www.quanser.com.

Schroeder, M.R. (1970), "Synthesis of low-peak-factor signals and binary sequences with low autocorrelation", *IEEE T. Inform. Theory*, **16**(1), 85-89.

Sonin, A.A. (1997), *The physical basis of dimensional analysis*, Department of mechanical engineering of Cambridge.

FC